Heliyon 10 (2024) e29296

Contents lists available at ScienceDirect

Heliyon

journal homepage: www.cell.com/heliyon

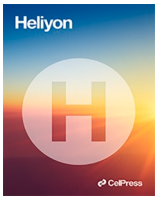

Research article

Scallop shells as biosorbents for water remediation from heavy metals: Contributions and mechanism of shell components in the adsorption of cadmium from aqueous matrix

Tatiana Chenet [a,*], Gunnar Schwarz [b], Christoph Neff [b], Bodo Hattendorf [b], Detlef Günther [b], Annalisa Martucci [c], Mirco Cescon [d], Andrea Baldi [d], Luisa Pasti [a]

[a] Department of Environment and Prevention Sciences, University of Ferrara, Via Borsari, 46, 44121, Ferrara, Italy
[b] Laboratory of Inorganic Chemistry, ETH Zürich, Vladimir-Prelog-Weg, 1, 8093, Zürich, Switzerland
[c] Department of Physics and Earth Science, University of Ferrara, Via Saragat, 1, 44122, Ferrara, Italy
[d] Department of Chemical, Pharmaceutical and Agricultural Sciences, University of Ferrara, Via Borsari, 46, 44121, Ferrara, Italy

ARTICLE INFO

Keywords:
Scallop shells
Biosorbents
Heavy metals
Adsorption
Water remediation
LA-ICPTOFMS

ABSTRACT

To ascertain their potential for heavy metal pollution remedy, we studied the adsorption mechanism of cadmium onto scallop shells and the interactions between the heavy metal and the shell matrix. Intact shells were used to investigate the uptake and diffusion of the metal contaminant onto the shell carbonatic layers, as well as to evaluate the distribution of major and trace elements in the matrix. LA-ICPMS measurements demonstrate that Cd is adsorbed on a very thin layer on the inner and outer surfaces of the shell. Structural and thermal analyses showed the presence of 9 wt.-% of a $CdCO_3$ phase indicating that the adsorption is mainly a superficial process which involves different processes, including ion exchange of Ca by Cd. In addition, organic components of the shell could contribute to adsorption as highlighted by different metal uptake observed for shells with different colours. In particular, darker shells appeared to adsorb more contaminant than the white ones. The contribution of the organic shell components on the adsorption of heavy metals was also highlighted by the element bulk content which showed higher concentrations of different metals in the darker specimen. Raman spectroscopy allowed to identify the pigments as carotenoids, confirmed by XRD measurements which highlighted the presence of astaxanthin phases. The results presented here provide new insights into the Cd adsorption mechanism highlighting the important contribution given by the organic components present in the biogenic carbonate matrix. Furthermore, the high efficiency of Cd removal from water by scallop shells, supported by adsorption kinetic and isotherm studies, has been demonstrated.

1. Introduction

Environmental pollution caused by heavy metals is one of the major global problems leading to adverse effects on ecosystems, biodiversity, and human health [1]. Among the heavy metals, cadmium (Cd) is one of the most toxic pollutants even at low concentrations. Furthermore, Cd has been classified as human carcinogen by the International Agency for Research on Cancer [2]. The main source of Cd pollution in surface waters is anthropogenic. On a global scale, smelting of non-ferrous metal ores has been regarded

* Corresponding author.
E-mail address: tatiana.chenet@unife.it (T. Chenet).

https://doi.org/10.1016/j.heliyon.2024.e29296
Received 11 July 2023; Received in revised form 5 March 2024; Accepted 4 April 2024
Available online 5 April 2024

as the largest anthropogenic source of Cd for the aquatic environment [3]. Cd tends to accumulate in the sediments by adsorption or precipitation as insoluble salts [4]. However, under certain conditions Cd can be mobilised and its concentration in the aqueous medium can increase. This is particularly the case when the salinity of the water body increases, and dissolved Cd is stabilised in solution through the formation of chloro-complexes [5].

Among the most common physical and chemical approaches for the removal of heavy metals from water, adsorption is an effective and economic technique, offering flexibility in the design and operation, and a vast variety of adsorbent materials [6–10]. In the last years, the use of natural or waste materials as adsorbents has been widely studied to favour eco-friendly approaches in environmental remediation applications [11]. Among the waste products generated by food industry, mollusc shells appear to have composition and structure characteristics which are suitable for the removal of heavy metals dissolved in water bodies.

In fact, many studies had reported the capability of molluscan or crustacean shell powder to adsorb heavy metals from water aqueous matrices considering the effect of the adsorbent grain size [12–14], different $CaCO_3$ shell structure [15], or after the adsorbent material had been acid-pretreated [16] or calcined [17–19]. It has been demonstrated by Tudor et al. (2006) [20] that some seashells are more efficient in the uptake of Pb and Cd compared to non-biogenic calcareous materials. Mollusc shells can also be employed as marine sediment amendments for immobilisation of potentially toxic elements, in this way the water and sediment quality would be improved without introducing extraneous materials in the lagoon system, since they are native of the area of interest. Furthermore, adding biogenic carbonate in marine sediments could possibly mitigate the effect of sea acidification, as suggested by Drylie et al. [21]. The use of mollusc shells for environmental remediation can contribute to improve the sustainability of shellfish farms since they are classified as waste material, and as such they require adherence to applicable policies and procedures to be correctly disposed [22]. In addition, the accumulation of heavy metals in mollusc shells ca be an important environmental indicator for evaluating water pollution by these contaminants; their concentrations in shells provide a time-integrated degree of metal availability, over long periods of time, thus providing an archive of past seawater. Therefore, shells can provide a more precise symptom of pollution and environmental change than soft tissue, due to the possibility of investigating the incorporation of elements over time of shell formation [23–26], higher preservation potential even after the organism's demise, and relatively cheap and easy storage. Besides, the lower metal concentrations in the shells with respect to soft tissue can be overcome by the development of sensitive analytical techniques [27,28].

The evaluation of the interactions of dissolved metal contaminants with the mollusc shell matrix and its components would provide additional information on the mechanism of the metal uptake process and can contribute to the development of the use of shells as bioadsorbents and bioindicators in environmental remediation and monitoring fields, respectively.

Herein, we present a study on the investigation of the mechanism of Cd adsorption and diffusion in the scallop shell carbonatic layers employing different analytical techniques, considering the interaction of heavy metals not only with the carbonate phase, but also with organic components present in the matrix. To detect the spatial distribution of trace elements contents, laser ablation inductively coupled plasma mass spectrometry (LA-ICPMS) has been employed. LA-ICPMS allows to determine the element distribution across heterogeneous and multiphase solid samples with low μm spatial resolution. In this work, LA was applied in combination with ICP-TOFMS, which allows fast and quasi-simultaneous detection of most elements having m/z in the range 7–238 [29,30], and the determination of element distributions on selected areas of the cross section of mollusc shells. Furthermore, it provides short analysis times with minimal sample preparation required [31] and by using LA-ICPTOFMS in the line scan mode, continuous element profiles of the sample can be measured. Many studies employed this technique to obtain natural trace elements patterns along the shell direction of growth in order to use them as proxies to retrace variations of temperature and salinity of the water body [32–37]. Despite the proven applicability of LA-ICPMS in line scan mode for retrospective natural trace elements monitoring, only few works applied this technique to investigate metal contaminants in mollusc shells [23,25,38,39] and, to the best of our knowledge, there is no study relating to the diffusion of the metal through the shell layers in mollusc shell treated with contaminants.

Since it has been demonstrated that the adsorption of metal can induce structural modification in the crystalline components of shells [40], thermogravimetric and X-ray powder diffraction analyses were carried out. The preliminary results indicate that scallop shells having different colourations show differences in Cd adsorption characteristics. This finding motivated us to investigate the role of pigments through micro-Raman and LA-ICP-TOFMS imaging [30].

The insights gathered from this study provide information to better understand the distribution and interactions of metal contaminants with the shell matrix when mollusc shells are used as adsorbents or environmental indicators.

2. Materials and methods

2.1. Adsorbent material preparation

One hundred scallop shells (Aequipecten opercularis, Linnaeus 1758) were collected from a shell deposal site in Sacca di Goro (Northern Adriatic Sea, Italy). The shells were first brushed to remove any residual mollusc tissue, cleaned thoroughly with deionised MilliQ water (Millipore, MA, USA) and then dried in an oven at 50 °C over night.

A total of 50 shells were selected and milled using a grinder (Retsch GmbH, Germany) to obtain a fine powder which was used for the determination of the mean calcium (Ca) content, particle size distribution, Cd adsorption experiments for kinetics and isotherm determination, and for thermal and X-ray powder diffraction analyses.

The material characterisation regarding minor and trace elements bulk composition was performed on scallop shells with different colouration, milled separately into a fine powder.

28 shells were kept intact and sorted by colour (white, pink and brown) for the metal diffusion investigation by LA-ICP-TOFMS and for pigment characterisation with micro-Raman spectroscopy.

For the overall experimental workflow see Supplementary Fig. S1 in the Supplementary Information.

2.2. Characterisation

The particle size distribution of the scallop shell powder used for batch adsorption experiments was determined with a Malvern Mastersizer 2000 Particle Analyser (Malvern instruments, UK).

For the determination of the bulk concentration of Ca, 0.1 g of scallop shell powder was digested in 10 mL of HNO_3 10 % (prepared from HNO_3 Fluka, analytical grade, purified by double subboiling distillation), filtered with PVDF membrane 0.45 μm (ACRODISC, New York, USA), diluted and analysed by solution based ICP-OES (PerkinElmer, Waltham, MA, USA) (for the measuring parameters see below in the *Batch adsorption* section).

To determine the trace elements bulk composition, three scallop shells were sorted by colour, milled into a fine powder, digested in HNO_3 10 %, then filtered using syringe filters with PVDF membrane 0.45 μm (ACRODISC, New York, USA). After dilution, the analyses were carried out using an Agilent 7500 ICP-QMS (Agilent Technologies, Santa Clara, CA, USA); the instrument operating parameters were: 1450 W RF power, 4.2 mm sampling depth, 15 L min^{-1} coolant gas, 1.00 L min^{-1} carrier gas, the isotopes measured were ^{25}Mg, ^{39}K; ^{49}Ti, ^{51}V, ^{55}Mn, ^{56}Fe, ^{59}Co, ^{62}Ni, ^{65}Cu, ^{66}Zn, ^{88}Sr, ^{107}Ag, ^{111}Cd, ^{113}Cd, ^{137}Ba, and ^{208}Pb.

2.3. Batch adsorption

Cd solutions were prepared by dissolving $Cd(NO_3)_2{\cdot}4H_2O$ (purity 99.997 %, Sigma-Aldrich, Steinheim, Germany) in ultrapure water (Millipore, MA, USA). The adsorption kinetics and isotherm were determined using the batch method, as explained below in the respective sections.

The Cd uptake at any time t for kinetic experiments (q_t) and at equilibrium for isotherm determination (q_e) was calculated with equations (1) and (2), respectively:

$$q_t = \frac{(C_0 - C_t) \bullet V}{m} \tag{1}$$

$$q_e = \frac{(C_0 - C_e) \bullet V}{m} \tag{2}$$

where q_t and q_e (mg g^{-1}) are the quantities of Cd adsorbed, C_0 (mg L^{-1}) is the concentration of Cd in the initial solution, C_t (mg L^{-1}) is the residual concentration at a time t in kinetic experiments, C_e (mg L^{-1}) the residual Cd concentration at equilibrium for isotherm determination, V (L) the volume of the solution in the batch, and m (g) the quantity of scallop shell powder.

2.3.1. Adsorption kinetics

The kinetic experiments were conducted at three different initial Cd concentrations (5, 10 and 15 mg L^{-1}), 1 L of solution was prepared in a polypropylene bottle where 5 g of shell powder was added. The batches were continuously stirred at a temperature of 21.0 ± 0.5 °C using a refrigerating bath circulator (Jeio Tech, Daejeon, Republic of Korea). Samples (0.5 mL) were collected at different time intervals: every minute for the first 10 min, every 5 min up to 1 h, every 30 min up to 3 h, and every 60 min up until 5h. The samples were filtered using 25 mm syringe filters with PVDF membrane and a pore size of 0.45 μm (Agilent Technologies, Santa Clara, CA, USA). Then the Ca and Cd residual concentration in the solution was evaluated by ICP-OES Optima 3100XL (PerkinElmer, Waltham, MA, USA) (axial view) equipped with a solid-state charge-coupled device detector (CCD), a peristaltic pump and a low-flow GemCone nebuliser coupled to a cyclonic spray chamber. Analytical lines 317.933 nm and 226.502 nm were selected for quantitative determination of Ca and Cd, respectively. The ICP-OES measuring parameters were: 15 L min-1 plasma flow, 0.5 L min-1 auxiliary flow, 0.65 L min-1 nebuliser flow, 1350 W RF power.

2.3.2. Adsorption isotherm

20 mL of Cd^{2+} solution were added to crimp top reaction glass flasks sealed with PTFE septa (Supelco, Bellefonte, PA, USA) with 40 mg of shell powder. The initial concentrations of Cd^{2+} in the solutions were in the range of 1–350 mg L^{-1}.

Adsorption experiments were performed with a contact time of 20 h, which is considered sufficiently longer than the equilibration time (30 min) as determined in the adsorption kinetics experiments.

After 20 h equilibration under stirring (600 rpm) and at a controlled temperature of 21.0 ± 0.5 °C, the adsorbent was separated from the solution by filtration using 25 mm syringe filters with PVDF membrane and 0.45 μm pore size (Agilent Technologies, Santa Clara, CA, USA) and the pH of the solution was recorded for each solution.

The concentration of Ca^{2+} and Cd^{2+} in the solution, before and after the contact with the adsorbent material, was determined by ICP-OES, as described before.

The same procedure was followed to obtain the adsorption isotherm of Cd onto commercial pure calcium carbonate powder (purity 98 %, Sigma-Aldrich, Steinheim, Germany).

2.4. Cd uptake across shell layers

For the study of the metal diffusion through the shell layers, the intact mollusc valves were put in contact with solutions containing

Cd^{2+}, the concentrations of the metal ions were 1.0 and 5.0 mg L^{-1}. After a contact time of 20 h to ensure that the equilibrium had been reached, the shells were separated from the solution, rinsed twice with ultrapure water, air-dried and conserved for the LA-ICPTOFMS experiments.The Cd concentration in the solution before and after the contact with the shells was measured by ICP-OES (for the measurement parameters see *Adsorption kinetics* section) and the Cd uptake was calculated (equation (2)).

To investigate the diffusion of Cd through the sample cross section, the shells were cut along the axis

of maximum growth with a low-speed saw (Isomet 11–1180 Low Speed Saw, Buehler LTD, Switzerland), embedded into an epoxy resin (Epofix, Struers, Birmensdorf, Switzerland), ground to the desired thickness with a polishing machine (Forcipol 1V Grinder Polisher, Metkon, Turkey) equipped with a 120 grit diamond disc, then polished with 600 and 800 grit SiC powder. In order to obtain the trace elements distribution through the shell layers, laser ablation was conducted on the cross-sections of the samples, with the ablation direction oriented perpendicular to the direction of shell growth, from the outer to the inner surface layer (Supplementary Fig. S2).

The high-resolution line scans and element imaging analyses were conducted with a 193 nm ArF Eximer laser system (GeoLas C, Lambda Physik, Germany) equipped with the parallel flow ablation cell [41] and was coupled to an ICPTOFMS (icpTOF2R, Tofwerk AG, Switzerland). Ablation spots with 5 μm diameter were used in an edge to edge arrangement. The imaging mode "hole drilling with cleaning pulse" was applied using the imaging control system according to Neff et al. [30]. The acquisition of one sampling position was conducted using one cleaning pulse which was not recorded, followed by 25 recorded laser pulses at 100 Hz repetition rate and a fluence of 15–20 J cm^{-2}. The ICP-TOFMS operating conditions were: 16 L min^{-1} plasma flow (Ar), 0.8 L min^{-1} auxiliary flow (Ar), 0.6–0.7 L min^{-1} make-up gas flow (Ar), 1.4–1.6 L min^{-1} carrier gas flow (He), 1400 W RF power. The carbonate reference material MACS-3 (U.S. Geological Survey, USA) was used as external standard and a 100 % mass normalisation approach [42] was applied for the quantification assuming all metals are present as carbonates. This assumption could lead to inaccuracy when real samples containing appreciable amounts of organic substances are analysed. In the present work, for instance the organic fraction is roughly 1 % (see *Structural and thermal analyses* section) and therefore the bias is not substantial. The isotopes ^{23}Na, ^{24}Mg, ^{44}Ca, ^{55}Mn, ^{56}Fe, ^{66}Zn ^{88}Sr, ^{114}Cd and ^{208}Pb were evaluated. The mass resolving power of 4500–5000 achieved by the icpTOF2R in the lower mass range (24–56 *m/z*) [43] allows to separate $^{24}Mg^+$ from $^{12}C_2^+$, $^{44}Ca^+$ from $^{12}C^{16}O_2^+$, $^{55}Mn^+$ from $^{40}Ar^{14}NH^+$, and $^{56}Fe^+$ from $^{40}Ar^{16}O^+$ and $^{40}Ca^{16}O^+$. Based on the ion signals recorded for the more abundant Sn-isotopes, interference of $^{114}Cd^+$ by $^{114}Sn^+$ was not observed and the higher abundance isotope could be used to maximize sensitivity and therefore to lower the limits of detection (LOD).

2.5. Micro-Raman analyses

Raman spectra were recorded with a LabRam HR800 micro-Raman instrument (Horiba Scientific, FR) equipped with a Peltier-cooled CCD detector at −70 °C, an Olympus BXFM microscope, a 600 groove/mm grating and a 50× objective to collect the Raman scattering signals. The excitation source was a He–Ne laser (632.8 nm line) with a maximum laser power of 20 mW. A minimum spectrum accumulation of 10 times per second was used; if a high background was recorded, the accumulations were increased to a maximum of 100 times per second to improve the signal-to-noise ratio.

2.6. Thermogravimetric analyses

Thermogravimetric analyses (TG) and differential thermal analysis (DTA) of both raw scallop shell powder and Cd-loaded scallop shell powder were performed on a thermal analyser (STA 409 PC LUXX, Netzsch, Germany). The measurements were carried out in air flow with a heating rate of 10 °C min^{-1} from room temperature to 1000 °C.

Table 1
Bulk composition (μg g^{-1}) with standard deviation (n = 5) and limit of detection (LOD) obtained from solution based ICP-MS analysis of powdered shells.

	White shell		Pink shell		Brown shell		LOD
	mean	SD	mean	SD	mean	SD	
Mg	92.8	1.3	76.9	0.8	106.8	0.9	0.17
K	1001	4	1189	6	1856	5	9.8
Ti	<LOD		<LOD		0.91	0.11	0.46
V	0.05	0.04	0.054	0.006	0.97	0.05	0.054
Mn	24.5	0.5	24.1	0.6	178	4	0.080
Fe	8.2	0.4	10.6	0.4	4766	9	0.22
Co	0.164	0.021	0.099	0.009	1.225	0.018	0.003
Ni	0.55	0.09	2.2	0.3	2.56	0.25	0.37
Cu	1.27	0.04	1.84	0.10	17.4	0.3	0.11
Zn	16.6	0.3	16.3	0.6	90.1	2.8	0.60
Sr	10134	6	947	9	10678	9	0.012
Ag	<LOD		<LOD		<LOD		0.036
Cd	0.24	0.11	0.30	0.09	0.54	0.17	0.17
Ba	1.74	0.11	1.90	0.07	8.4	0.4	0.080
Pb	0.78	0.04	0.69	0.06	3.56	0.08	0.030

2.7. X-ray powder diffraction

The X-ray powder diffraction patterns of scallop shell powder, both untreated and treated with Cd solution, were recorded on a diffractometer (D8 Advance, Bruker, USA) equipped with a Si (Li) solid-state detector (Cu $Ka_{1,2}$ radiation, 3–110 2θ range, counting time of 12 s per 0.02 2θ step). The unit cell parameters were refined together with the coefficients of the pseudo-Voigt function modelling the profile function of the Bragg peaks and of the function modelling the background (a six-term cosine Fourier series). Refinements were carried out by the Rietveld method using the GSAS [44] and EXPGUI [45] packages. Structural models for all the phases were taken from the ICSD database [46]. Optimised parameters in final refinement were: background coefficients, cell parameters, zero shift error, peak shape parameters, preferred orientation, and phase fractions.

3. Results and discussion

3.1. Adsorbent material characterisation

The bulk composition of the shells was determined to evaluate the total cation contents of the untreated shells. The mass fractions determined by ICP-MS after acid digestion of ground shells are reported in Table 1. Many metals, in particular V, Mn, Fe, Co, Cu, Zn, Ba, and Pb were detected above the limits of detection in the samples. Among these, Fe was the most abundant element in the brown shell. The mass fractions of Cd were between the limit of detection and quantification of the employed method, thus indicating that the metal may be present in very low concentrations in the environmental habitat of these seashells, or that the replacement of Ca^{2+} in the calcium carbonate structure during the shell formation occurs to a lesser extent. Indeed, bioaccumulation rate of ions from seawater seems to be a function of many environmental and biological factors [47–49], and different habitats, species, or even individual specimens at different stages of development, may present different patterns of metal uptake. Furthermore, only few published studies [50–53] deal with chemical composition of scallop shells and none of these in a habitat similar to that of the samples herein investigated (i.e., a lagoon on the Po River Delta). In this aspect, the present study on one hand can provide new data that can contribute to the knowledge on metal distribution in biota. On the other hand, the data cannot be compared with literature data.

Recently, the concentration of metals in sediments of Laguna di Goro have been investigated [54], and it has been found that trace-metals, such as Ni, Co, V and Cu, show concentration levels corresponding to the geological nature of the Po River alluvial

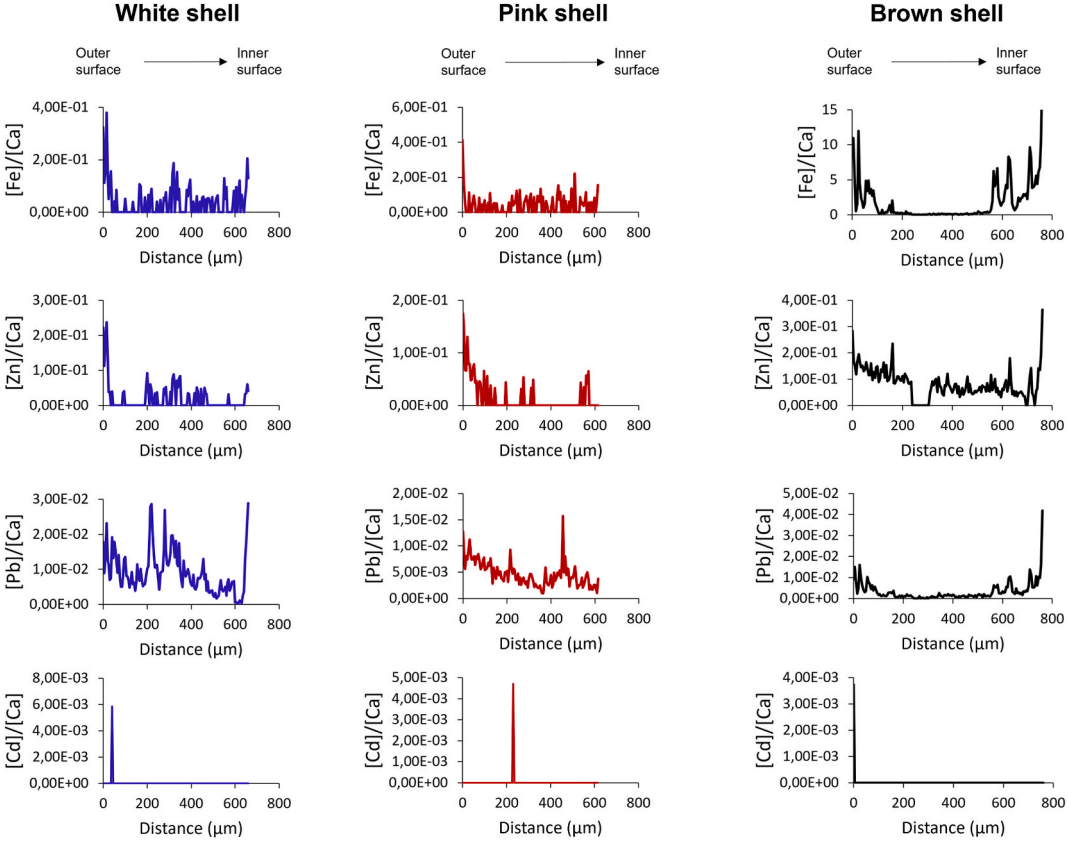

Fig. 1. Trace element concentration profiles expressed as element/Ca ratio (mmol mol^{-1}) obtained from LA-ICP-TOFMS line scan carried out on not treated scallop shells; (the x-axis ranges from the outer to the inner surface of the shells).

sediments, whereas Pb and Zn show an enrichment in Sacca di Goro, probably due to anthropogenic sources. Indeed, these trace-metals were found in all the scallop shell samples analysed.

A particular feature that can be observed from the elements bulk composition is the fact that whereas for heavy metals such as Pb, Fe and Zn there is a higher concentration in the darker coloured shell, the content of elements found naturally in the shells, such as Sr and Mg which are incorporated during the mollusc growth, does not vary so substantially between shells of different colouration. These findings suggest that the components responsible for the shell colouration contribute significantly to the uptake of heavy metals from the aqueous environment surrounding the mollusc.

To further investigate on the scallop shell composition, specimens of shells were analysed before the contact with solution of Cd^{2+}. Compositional trace elemental variability in biogenic carbonates can be assessed by static layer by layer removal of material to obtain a depth-compositional profile. Alternatively, it can be carried out by LA-ICP-TOFMS along a defined section oriented perpendicular to the accretionary growth direction [25]. The latter method was applied in the present study.

The investigation of the causes of the variability in the distribution of shell elemental components lays beyond the aim of this study, any correlation to seasonal environmental variations or pollution events cannot be made since the history of the shells, collected from a disposal site, is unknown. Nevertheless, information on the distribution of major and trace components of the shells used in this study can be obtained, highlighting the capability of the technique employed.

In Fig. 1, the profile of the ratios of trace elements (i.e., Fe, Zn, Pb and Cd) with respect to Ca [23,25,26] of three original scallop shell specimens are shown.

Lead was detected in every shell analysed, showing different distribution patterns across the shells, with peaks of higher abundance suggesting that during the formation of those layers, the organism was surrounded by a polluted environment.

Natali and Bianchini [54] reported that the sediments of Sacca di Goro are particularly enriched in Pb, with enrichment factors up to three with respect to the natural composition of alluvial sediments of the Padanian plain [55], taken as representative of the geogenic local background. The high Pb enrichment factor found in the lagoon sediments suggests anthropogenic contributions, possibly related to atmospheric emissions [54]. Similar behaviours were found for Fe and Zn in the shells analysed, possibly related to the composition of the alluvial sediments [56]. Regarding the metal contaminant considered in the present work, Cd/Ca concentration profiles for the three shells before treatment show that Cd concentration across the shell layers is below the LOD; therefore, the results on the contaminant distribution obtained after the treatment of the shells with Cd-containing solution (see below) are entirely ascribable to the treatment performed.

In Supplementary Fig. S3 the profile of the ratios of Na, Mg and Sr with respect to Ca of three different specimens is reported. Variations in compositions could originate from shells growth [24]. These ratios, generally reported as mmol mol^{-1} [34,57], are biogeochemical parameters reflecting the Earth–ocean–atmosphere dynamic exchange of elements [58] and are commonly employed to investigate trace elemental and isotopic inventor in successively secreted carbonate layers related to past environmental conditions of seashells [58].

Generally, there is variability for all three elements in the element/Ca between the scallop shells, even though they belong to the same species. In addition, variations were observed within the same shell across the different regions (see the profiles of Na/Ca of all the three shells and Mg/Ca of the brown shell). Regarding strontium, the Sr/Ca profiles were characterised by distinct variations, especially in the white and brown specimens, suggesting an alteration in the incorporation rate of this element during the shell layers deposition, possibly related to seasonal temperature variations which most likely influence the shell calcification and hence the Sr/Ca ratio [50,59].

Moreover, the brown shell shows a significant variation of the content of all three elements in a region between 230 and 315 μm; in particular, Mg decreases while Na and Sr increase. The investigation of the causes that led to this particular variation is beyond the aim of the present study, and correlations with seasonal variations cannot be made since the history of the shell is unknown. Nevertheless, such alteration in the distribution of these major components suggests that the mollusc was subjected to a stress condition that possibly led to an alteration in the metabolic processes or of the growth rate, resulting in a different incorporation of these elements during the formation of the shell [50,59].

3.2. Adsorption of Cd from aqueous solution onto powdered scallop shells

In this work, we focus on the interaction of Cd on surface scallop shells. However, to quantify the adsorption of this material for the comparison with literature data, adsorption experiments on powdered scallop shells were carried out as well. The aim of these experiments was to investigate the capability of the powdered shell to adsorb Cd from solution. The kinetics and thermodynamics of adsorption can depend on particle dimensions, but in this study we were rather focusing on the mechanisms of the adsorption instead of on maximising the adsorption capability.

In order to evaluate the adsorption properties of powdered scallop shells employed in the present study, the kinetics and thermodynamics of the adsorption process were investigated. Details of the obtained results are reported in the Supplementary Information.

The experiments were carried out with powdered scallop shells characterised by particle dimensions spanning over a broad range, with an average value of 15 μm (see Supplementary Fig. S4).

The adsorption properties of shells towards Cd^{2+} were evaluated at pH 7.0–8.5, measured at the end of the equilibration time of the batch experiments to account for shells dissolution (see Supplementary Discussion S1). The experiments were conducted at two temperatures, 21.0 ± 0.5 °C and 9.0 ± 0.5 °C, the latter to mimic seawater temperature range in the region more closely.

3.2.1. Adsorption kinetics

The adsorption kinetics was investigated in a series of experiments for which the uptake was measured at different contact times.

The adsorption kinetics obtained at three different initial concentrations are reported in Fig. 2a.

The adsorption was very fast, with the equilibrium reached within 30 min, and the majority of Cd removed in the first 15 min, for all the initial concentrations considered. These results are comparable with those found by Jeon [60] for the adsorption of Cd onto grinded pen shells.

The very fast Cd uptake highlights the applicability of scallop shells as adsorbents in water remediation technologies; moreover, the short time needed for reaching equilibrium makes this material suitable also for continuous flow systems [61].

The experimental data were fitted with different kinetics models; the pseudo second order (PSO) kinetic model [13,18,62] is described by equation (3):

$$q_t = \frac{k_2 \bullet q_{eq}^2 \bullet t}{1 + k_2 \bullet q_{eq} \bullet t} \tag{3}$$

Where q_t (calculated using eq. (1)) is the amount of Cd adsorbed at time t, q_{eq} is the quantity adsorbed when the equilibrium is reached, and k_2 the pseudo second order rate constant.

The pseudo first order (PFO) kinetic model is described as follows:

$$q_t = q_e \bullet \left(1 - e^{-k_1 \bullet t}\right) \tag{4}$$

Where k_1 is the pseudo first order rate constant.

The parameters obtained from the fitting are reported in Supplementary Table S1.

By comparison of the determination coefficients of the two models, the experimental data were better described by the PSO model. The good applicability of this model is usually associated with the situation when the rate of direct adsorption/desorption process

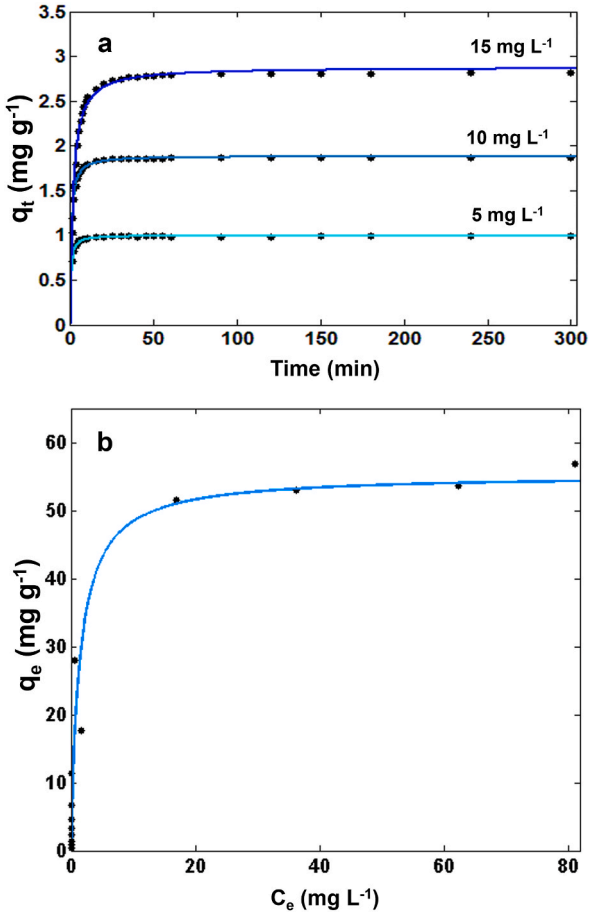

Fig. 2. a) Effect of contact time on the adsorption of Cd onto scallop shell powder at three different initial metal concentrations, experimental data fitted with the PSO kinetic model; b) Adsorption isotherm of Cd onto scallop shell powder (21 °C), experimental data fitted with the Langmuir isotherm model.

(seen as a kind of chemical reaction referred to as "surface reaction'') controls the overall sorption kinetics [63]; for further details see Supplementary Discussion S2.

3.2.2. Adsorption isotherm

The data obtained from batch experiments at the constant temperatures of 21 °C and 9 °C were fitted using two different models; the Langmuir isotherm model [64] is represented by the following equation:

$$q_e = \frac{q_{max} \bullet b \bullet C_e}{1 + b \bullet C_e} \quad (5)$$

where q_e (calculated using eq. (2)) is the amount of Cd adsorbed at the equilibrium (mg g^{-1}), C_e is the equilibrium concentration (mg L^{-1}), q_{max} is the saturation capacity of shell powder (mg g^{-1}) and b the adsorption constant (L mg^{-1}).

The Freundlich isotherm model [64] is described by equation (6):

$$q_e = K_F \bullet C_e^{1/n} \quad (6)$$

Where K_F is a constant related to the adsorption capacity ((mg g^{-1})(L g^{-1})^n) and n represents the adsorption intensity.

Fig. 2b shows the isotherm of Cd on scallop shell powder at 21 °C (see Supplementary Fig. S7 for the isotherm at 9 °C): the curve has a concave shape, and it is characterised by a steep initial zone and a saturation plateau. The shape of the isotherm indicates a favourable adsorption of the metal onto the adsorbent material. This information, together with the relatively fast adsorption kinetics (see above), confirms that scallop shell is a promising adsorbent for Cd. The parameters obtained from the numerical fit are listed in Supplementary Table S2; the higher R^2 values obtained with the Langmuir model compared to the Freundlich model indicate the former as the better choice for the description of the experimental data.

The Langmuir isotherm model refers to homogeneous adsorption without taking in consideration adsorbate-adsorbate and adsorbate-solvent interactions; furthermore, the adsorption sites are energetically equivalent.

Moreover, the saturation capacity of the scallop shell powder (55 mg g^{-1}, SD 7 mg g^{-1}) is significantly higher compared to that obtained with pure calcium carbonate powder (12.8 mg g^{-1}, SD: 1.6 mg g^{-1}, see Supplementary Fig. S8) demonstrating that the composition of the biogenic shell matrix significantly enhances the capability of removing Cd from water matrices.

3.3. Structural and thermal analyses

The mineral phases occurring in scallop shells were identified by examination of XRD patterns. Qualitative mineralogical analysis revealed that calcite was present in all the analysed samples. The coexistence with otavite, $CdCO_3$, in the Cd-treated scallop shells can be inferred from inspection of the 20–60° **2θ** region (i.e. 2θ = 23.56, 30.35, 36.52, 43.92, 49.60 50.02°) showing the increased complexity of the diffraction pattern of samples containing two carbonates with respect to sample with only calcite (Fig. 3). Consequently, the process involved in Cd uptake by calcite was adsorption and Cd diffusion into the calcite crystal, leading to the formation of $(Cd_xCa_{1-x})CO_3$ solid-solution. At the same time, the occurrence of otavite in the Cd-loaded Scallop shells sample indicated that shell calcite substrate immersed in aqueous solutions containing Cd^{2+} acted also as passive surface, leading to dissolution of calcite and nucleation of otavite [65]. Finally, polyenes (i.e. astaxanthin) [66,67], were identified based on the weak reflections in the 20–35° 2θ range (i.e. 2θ = 18.2, 20.5, 22.7, 25.5 and 32.2°) in Cd-scallop shells. This result is in good agreement with the Raman spectra indicating the presence of a low fraction of pigments increasing the Cd adsorption efficiency of the biogenic $CaCO_3$ compared to geologic one [68,69].

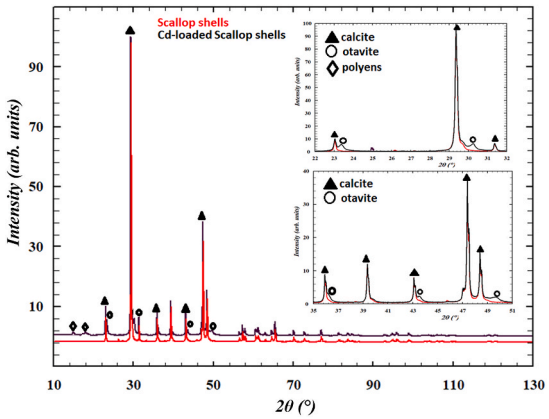

Fig. 3. Comparison between XRD patterns of scallop shells (red line) and Cd-scallop shells (black line) respectively. (For interpretation of the references to colour in this figure legend, the reader is referred to the Web version of this article.)

In order to quantify the phases content in Cd-loaded Scallop shells, quantitative phase analysis (QPA) by use of the Rietveld method was performed. It is well known that this approach gives rise to more accurate values compared to any other single technique, such as Fourier transform infrared spectroscopy (FTIR), chemical analysis and electron microscopy [70].

In this procedure, the weight fraction w*i* of each *i*th crystalline component in the multiphase system is calculated from the corresponding refined scale parameter *Si*, according to the equation:

$$wi = \frac{SiMiVi}{\sum_j SjMjVj} \quad with\ the\ normalisation\ condition \sum wi = 1.0 \tag{7}$$

with *Mi* and *Vi*, the unit cell mass and volume, respectively [71]. Firstly, quantitative refinement was performed by assuming calcite as the only carbonate present in scallop shells. In Cd-treated samples, the quantitative refinement was including both otavite and astaxanthin; the mass fractions obtained by Rietveld refinements are 90 wt% calcite, 9 wt% otavite and 1 wt% astaxanthin.

In addition, a correlation between the refined unit cell parameters of calcite and the Cd incorporation was noted (Table 2). In order to explain these variations, we suggest that in our samples the compression of the refined unit cell volume can be mainly ascribed to an increase of the Cd content due to the smaller ionic radius of Cadmium (0.95 Å) with respect to Calcium (1.06 Å) [72].

The trend of DTA and TG curves for both scallop shells samples are represented in Fig. 4. Below 100 °C, DTA curves showed an endothermic peak weakly indicating low amounts of absorbed water. The occurrence of otavite was confirmed by a broad endothermic peak between about 370 and 460 °C due to the decomposition of $CdCO_3$ into CdO under atmospheric pressure [73,74]. In the same temperature range the polyenes' decomposition also occurred [67,75]. Endothermic effects in the 720–900 °C temperature range are ascribable to the CO_2 releasing by $CaCO_3$ decomposition. Lastly, the exothermic peak above 900 °C can be interpreted as the crystallisation of newly formed minerals.

The adsorption experiments performed using powdered scallop shells illustrated above were carried out to determine the mean values of Cd uptake obtained for a given particle distribution. To investigate the contaminant distribution and interactions with the shell matrix, intact scallop shell valves were used.

3.4. Cd distribution after adsorption

To study the distribution of the metal contaminant through the shell layers, Cd profiles were obtained from scallop shells treated with aqueous solutions containing Cd. Since scallop shells of different colours showed differences in composition, we selected scallop shells with three different colourations (white, pink and brown) to investigate potential differences in Cd adsorption characteristics. The colouration of mollusc shells is mainly due to the presence of organic pigments, mostly tetrapyrroles, carotenoids and melanins [76]. Not only the colour and pattern of shells vary between species, but different colouration can also occur among a single species, or even a single shell can present differently coloured areas [77].

In Fig. 5 the Ca and Cd distribution profiles of three scallop shell samples, white, pink and brown, treated with Cd solution, are reported. Calcium carbonate ($CaCO_3$) consists of 40.0 % calcium. The profiles indicate that Ca, mainly present as calcium carbonate, is the main component of the shells. Slight variations of the Ca content were observed and have been already reported for Ca in bivalves [78]. Generally, they can be related to seashell metabolic variations or different environmental conditions.

The Cd profiles of the three specimens show the metal distribution, with highest concentrations on a thin layer located on the surfaces of the shell. Most of the adsorbed Cd was detected within the first 10 μm on both the inner and outer surface. A minor concentration of Cd is found in the first 50 μm towards the internal layers on both the boundary surfaces.

In the distribution profiles shown in Fig. 5 the Cd concentrations on the shell surfaces are similar for the white and brown shells, whereas they are much higher for the pink one; it should be noted however that these profiles refer to a very thin shell section (5 μm wide) and thus they are not representative of the entire shell. To better investigate the differences in the Cd uptake of the different coloured shells, bulk concentrations should be considered. The Cd distribution profiles were determined to evaluate the metal distribution into the adsorbent.

3.5. Cd bulk concentration and micro-Raman

To further investigate the role of shell pigment on adsorption, batch experiments were carried out by using scallop shells with three different colourations (white, pink and brown). As reported in Fig. 6, the Cd uptake (q_e) is lower for the white shells and it increases for

Table 2
Refined unit cell parameters for scallop shells not treated and scallop shells treated with solution containing Cd.

Scallop shells						
Calcite	Space Group	a (Å)	c(Å)	α = β(°)	γ(°)	Volume(Å^3)
	$R\,\bar{3}\,c$	4.9987(1)	17.1099(3)	90	120	370.24(1)
Cd-loaded Scallop shells						
	Space Group	a(Å)	c(Å)	α = β(°)	γ(°)	Volume(Å^3)
Calcite	$R\,\bar{3}\,c$	4.9981(2)	17.1109(5)	90	120	370.18(2)
Otavite	$R\,\bar{3}\,c$	4.9642(2)	16.2980(8)	90	120	347.83(3)

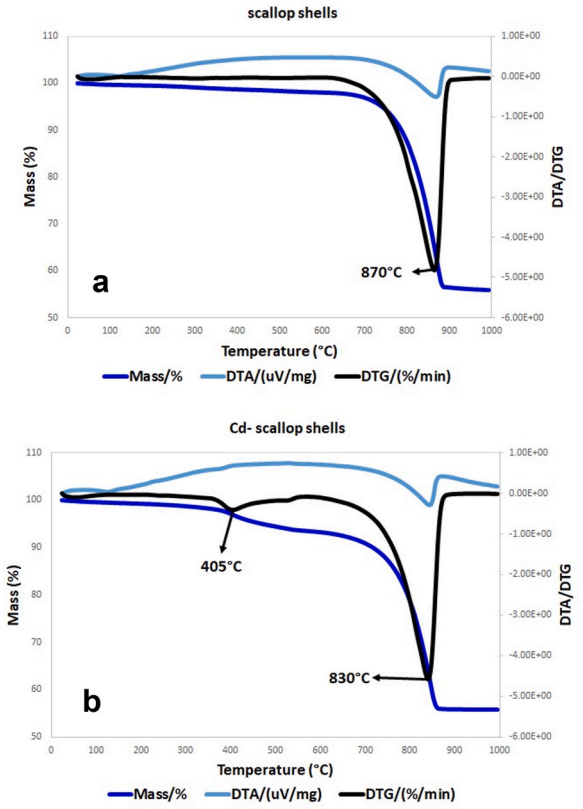

Fig. 4. Comparison between TG, DTG and DTA curves of scallop shells (a) and Cd-scallop shells (b) one in the 25–1000 °C temperature range, respectively.

the pink and brown shells, with the latter showing the highest uptake values. The variation in metal adsorption is more evident when the Cd concentration in the aqueous solution increases (Fig. 6b), especially between white and brown shells. A two-way analysis of variance (ANOVA) was applied to the adsorption data. It can be seen in Table S3 of the Supplementary information that the Cd uptake shows significant differences ($F_{crit} < F$) as a function of the initial metal concentration in solution and shells with different colouration.

These findings suggest that the components of the shell matrix responsible for its colouration enhances the metal adsorption. Evidence of the higher uptake of metals by the coloured shells rather than the white ones is also accentuated by the bulk concentration analyses (Table 1) which showed higher content of many metals, including Fe, Cu, Zn, and Pb, in the pink and especially in the brown shells.

To examine in depth this particular feature, we investigated the nature of the pigments contained in our samples employing the micro-Raman technique [77,79–81].

In Fig. 7 the Raman spectra acquired on the outer surface of scallop shells presenting different colours are reported. The white shell spectrum (Fig. 7a) presents only the bands at 1083, 707 and 274 cm^{-1}, belonging to the calcite matrix, while the spectra of the pink and brown samples (Fig. 7b and c, respectively) show two more bands, with higher intensities for the darker shells. The bands observed at ca. 1120 and 1500 cm^{-1} can be attributed to the stretching modes of the C═C double bond (ν_1) and the C–C single bond (ν_2) due to the presence of molecules characterised by a polyacetylenic chain [77,79,82]. In the Raman spectrum of the brown shell, we observed to more bands with much lower intensity at 1010 cm^{-1} and 1292 cm^{-1}, the former can be attributed to the CH═CH out-of-plane wagging mode (ν_4) and the latter to the CH═CH in-plane rocking mode (ν_3) [77].

The use of micro-Raman technique allowed us to identify the nature of the scallop shell pigments as polyenes, possibly belonging to the class of carotenoids by comparison with literature spectra [77,79–81]. The presence of these components in the carbonate matrix results in the enhancement of the adsorption efficiency of the biogenic $CaCO_3$ towards Cd compared to commercial $CaCO_3$ [20]. This result is in good agreement with the XRD data indicating the presence of a low fraction of pigments increasing the Cd adsorption efficiency of the biogenic $CaCO_3$ compared to geologic one [68,69]. Indeed, the metal cation chelating capacity of the carotenoid astaxanthin has been proven [83,84].

3.6. Summary

The current work focused on the study of the mechanism of adsorption of the heavy metal cadmium onto scallop shells; in

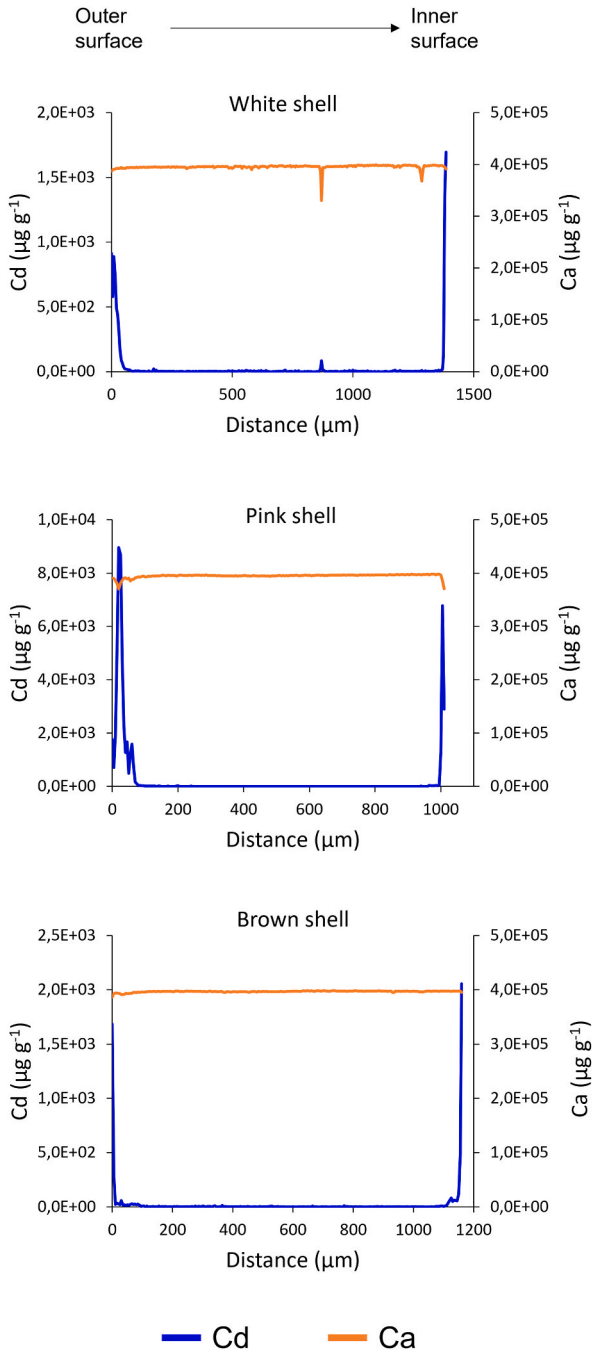

Fig. 5. Cd and Ca concentration profiles of the cross section of three scallop shells treated with 1 mg L^{-1} Cd solution.

particular, the interactions between the metal and the components of the shell matrix were evaluated.

The bulk composition of shells taken from a deposit site was determined with regards to their colouration. In general, the brown shell showed higher amounts of Mn, Fe, Co, Cu, Zn, Ba, and Pb than the white and pink ones; regarding the contaminant investigated, Cd content was close to the limit of quantification of the method, indicating that the environment in which the shells were collected was not severely polluted by Cd.

LA-ICP-TOFMS was employed to investigate the spatial distribution of major components and trace metals along the shell cross-section; Na, Mg and Sr showed minor variability between the different shells and within the layers of the same shell; in particular, Sr showed distinct layers with different Sr concentration parallel to the surface, possibly correlated to environmental factors such as temperature. Trace metals, such as Fe, Zn and Pb showed variations in their distribution across the shells cross section, especially for

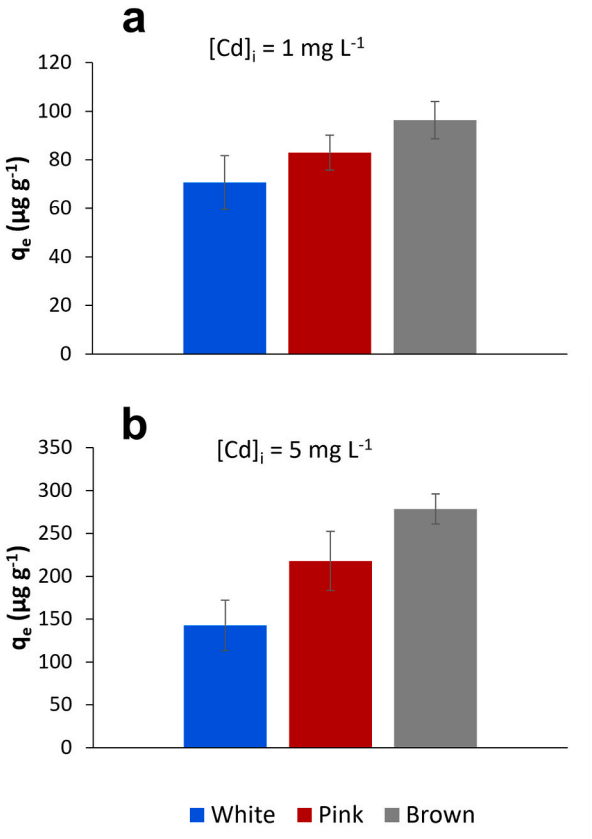

Fig. 6. Cd uptake (q_e) with standard deviation (n = 3) of scallop shells with different colouration treated with 1 mg L^{-1} (a) and 5 mg L^{-1} (b) Cd aqueous solution.

the brown specimen.

Powdered scallop shells, with an average particle dimension of 15 μm, were employed to investigate the capability to adsorb Cd. The kinetic experiments highlighted that the adsorption is a very fast process, reaching the equilibrium within the first 30 min.

The determination of the adsorption isotherm, obtained at 9 and 21 °C, allowed to determine the saturation capacity of the material which resulted to be temperature dependent. In particular, at 21 °C the saturation capacity was found to be significantly higher than that obtained using commercially available $CaCO_3$ powder.

The analysis of XRD patterns of the scallop shell powder before and after Cd adsorption showed that the material is mainly composed of calcite, while, after the contact with the Cd containing solution, the presence of otavite ($CdCO_3$) phase was observed, whose presence was also indicated by DTA and TG analyses. These findings, in addition with the kinetic experiments where an increase of Ca concentration in solution was observed during the adsorption, demonstrate that the adsorption process involves mainly an ion exchange between Ca and Cd.

The distribution and interactions of the Cd contaminant with the shell matrix were investigated using intact shell valves sorted by colour. High-resolution LA-ICPTOFMS imaging allowed to assess Cd distribution after adsorption; an enrichment of Cd was found on a thin layer (10 μm) on both the inner and outer surfaces of the shell, with a minor Cd concentration found in the first 50 μm towards the internal layers.

For each shell, the total Cd uptake was evaluated: the white shells showed the lower Cd adsorption, while for the pink and brown shells the metal uptake increased, with the brown shells showing the highest adsorption values.

The nature of the pigments contained in the differently coloured shells was determined by micro-Raman spectroscopy; the Raman spectra showed the bands typical of polyenes, possibly carotenoids, as also highlighted by the astaxanthin phase present in the XRD patterns.

4. Conclusions

The results reported provide new information on the mechanism of adsorption of Cd onto biogenic $CaCO_3$. Structural and thermal analyses highlighted the presence of cadmium carbonate phases in the scallop shells treated with aqueous solutions containing the metal contaminant, indicating that the adsorption is predominantly a superficial process involving the partial dissolution of superficial

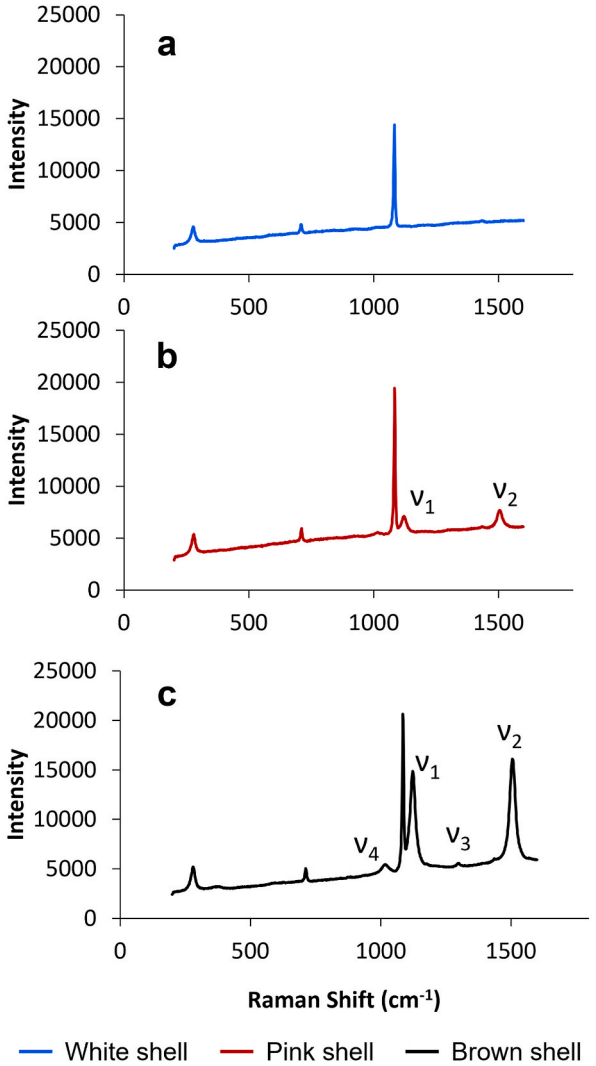

Fig. 7. Micro-Raman spectra of white, pink and brown shells. (For interpretation of the references to colour in this figure legend, the reader is referred to the Web version of this article.)

calcite and the nucleation of cadmium carbonate.

Cd is adsorbed on the inner and outer surfaces when intact scallop shells are used as adsorbent. The bulk concentration values showed that the metal adsorption depends on the mollusc species and on the quantity of organic substances (i.e., pigments) present in the carbonatic matrix. Indeed, we found higher cadmium uptake for scallop shells characterised by more intense and widespread colouration, even if the exchange with carbonate is the dominant adsorption mechanism. The pigments were identified as carotenoids, in particular, the XRD pattern showed the presence of astaxanthin phases which can act as complexing agent towards Cd, increasing its removal from aqueous media.

CRediT authorship contribution statement

Tatiana Chenet: Conceptualization, Data curation, Investigation, Visualization, Writing – original draft. **Gunnar Schwarz:** Conceptualization, Data curation, Investigation. **Christoph Neff:** Investigation, Conceptualization, Data curation. **Bodo Hattendorf:** Supervision, Writing – review & editing. **Detlef Günther:** Resources, Supervision, Writing – review & editing. **Annalisa Martucci:** Data curation, Investigation. **Mirco Cescon:** Investigation. **Andrea Baldi:** Investigation. **Luisa Pasti:** Funding acquisition, Resources, Supervision, Writing – review & editing.

Declaration of competing interest

The authors declare the following financial interests/personal relationships which may be considered as potential competing

interests: Luisa Pasti reports financial support was provided by MUR.

Acknowledgments

The research leading to these results has received funding from the University of Ferrara "Bando anno 2021 per progetti di ricerca finanziati con il contributo 5x1000 anno 2019" and from PNRR MUR project ECS_00000033_ECOSISTER.

Appendix A. Supplementary data

Supplementary data to this article can be found online at https://doi.org/10.1016/j.heliyon.2024.e29296.

References

[1] M. Jaishankar, T. Tseten, N. Anbalagan, B.B. Mathew, K.N. Beeregowda, Toxicity, mechanism and health effects of some heavy metals, Interdiscipl. Toxicol. 7 (2) (2014) 60–72, https://doi.org/10.2478/intox-2014-0009.
[2] Cadmium and cadmium compounds, IARC Monogr. Eval. Carcinog. Risks Hum. 58 (1993) 119–237.
[3] J. Pan, J.A. Plant, N. Voulvoulis, C.J. Oates, C. Ihlenfeld, Cadmium levels in Europe: implications for human health, Environ. Geochem. Health 32 (2010) 1–12, https://doi.org/10.1007/s10653-009-9273-2.
[4] J.L. Morford, S. Emerson, The geochemistry of redox sensitive trace metals in sediments, Geochem. Cosmochim. Acta 63 (11–12) (1999) 1735–1750, https://doi.org/10.1016/S0016-7037(99)00126-X.
[5] A. Dabrin, J. Schäfer, G. Blanc, E. Strady, M. Masson, C. Bossy, S. Castelle, N. Girardot, A. Coynel, Improving estuarine net flux estimates for dissolved cadmium export at the annual timescale: application to the Gironde Estuary, Estuar. Coast Shelf Sci. 84 (4) (2009) 429–439, https://doi.org/10.1016/j.ecss.2009.07.006.
[6] C.F. Carolin, P.S. Kumar, A. Saravanan, G.J. Joshiba, Mu Naushad, Efficient techniques for the removal of toxic heavy metals from aquatic environment: a review, J. Environ. Chem. Eng. 5 (3) (2017) 2782–2799, https://doi.org/10.1016/j.jece.2017.05.029.
[7] K. Naseem, R. Begum, W. Wu, M. Usman, A. Irfan, A.G. Al-Sehemi, Z.H. Farooqi, Adsorptive removal of heavy metal ions using polystyrene-poly(N-isopropylmethacrylamide-acrylic acid) core/shell gel particles: adsorption isotherms and kinetic study, J. Mol. Liq. 277 (2019) 522–531, https://doi.org/10.1016/j.molliq.2018.12.054.
[8] E. Nishikawa, S.L. Cardoso, C.S.D. Costa, M.G.C. da Silva, M.G.A. Vieira, New perception of the continuous biosorption of cadmium on a seaweed derivative waste, J. Water Process Eng. 36 (2020) 101322, https://doi.org/10.1016/j.jwpe.2020.101322.
[9] H. Huang, Q. Jia, W. Jing, H.U. Dahms, L. Wang, Screening strains for microbial biosorption technology of cadmium, Chemosphere 251 (2020) 126428, https://doi.org/10.1016/j.chemosphere.2020.126428.
[10] K. Naseem, Z.H. Farooqi, R. Begum, M.Z.U. Rehman, A. Shahbaz, U. Farooq, M. Ali, H.M.A.U. Rahman, A. Irfan, A.G. Al-Sehemi, Removal of cadmium (II) from aqueous medium using *Vigna radiata* leave biomass: equilibrium isotherms, kinetics and thermodynamics, Z. Phys. Chem. 233 (2019) 669–690, https://doi.org/10.1515/zpch-2018-1223.
[11] N.B. Singh, G. Nagpal, S. Agrawal, Rachna, water purification by using adsorbents: a review, Environ. Technol. Innov. 11 (2018) 187–240, https://doi.org/10.1016/j.eti.2018.05.006.
[12] S.J. Köhler, P. Cubillas, J.D. Rodríguez-Blanco, C. Bauer, M. Prieto, Removal of cadmium from wastewaters by aragonite shells and the influence of other divalent cations, Environ. Sci. Technol. 41 (1) (2007) 112–118, https://doi.org/10.1021/es060756j.
[13] Y. Du, L. Zhu, G. Shan, Removal of Cd2+ from contaminated water by nano-sized aragonite mollusk shell and the competition of coexisting metal ions, J. Colloid Interface Sci. 367 (1) (2012) 378–382, https://doi.org/10.1016/j.jcis.2011.10.023.
[14] F.A. Ismail, A.Z. Aris, Experimental determination of Cd2+ adsorption mechanism on low-cost biological waste, Front. Environ. Sci. Eng. 7 (2013) 356–364, https://doi.org/10.1007/s11783-013-0488-1.
[15] Q. Wu, J. Chen, M. Clark, Y. Yu, Adsorption of copper to different biogenic oyster shell structures, Appl. Surf. Sci. 311 (2014) 264–272, https://doi.org/10.1016/j.apsusc.2014.05.054.
[16] Y. Liu, C. Sun, J. Xu, Y. Li, The use of raw and acid-pretreated bivalve mollusk shells to remove metals from aqueous solutions, J. Hazard Mater. 168 (1) (2009) 156–162, https://doi.org/10.1016/j.jhazmat.2009.02.009.
[17] S. Peña-Rodríguez, D. Fernández-Calviño, J.C. Nóvoa-Muñoz, M. Arias-Estévez, A. Núñez-Delgado, M.J. Fernández-Sanjurjo, E. Álvarez-Rodríguez, Kinetics of Hg(II) adsorption and desorption in calcined mussel shells, J. Hazard Mater. 180 (1–3) (2010) 622–627, https://doi.org/10.1016/j.jhazmat.2010.04.079.
[18] D. Alidoust, M. Kawahigashi, S. Yoshizawa, H. Sumida, M. Watanabe, Mechanism of cadmium biosorption from aqueous solutions using calcined oyster shells, J. Environ. Manag. 150 (2015) 103–110, https://doi.org/10.1016/j.jenvman.2014.10.032.
[19] H.Y. Yen, J.Y. Li, Process optimization for Ni(II) removal from wastewater by calcined oyster shell powders using Taguchi method, J. Environ. Manag. 161 (2015) 344–349, https://doi.org/10.1016/j.jenvman.2015.07.024.
[20] H.E.A. Tudor, C.C. Gryte, C.C. Harris, Seashells: detoxifying agents for metal-contaminated waters, Water Air Soil Pollut. 173 (2006) 209–242, https://doi.org/10.1007/s11270-005-9060-3.
[21] T.P. Drylie, H.R. Needham, A.M. Lohrer, A. Hartland, C.A. Pilditch, Calcium carbonate alters the functional response of coastal sediments to eutrophication-induced acidification, Sci. Rep. 9 (2019) 12012, https://doi.org/10.1038/s41598-019-48549-8.
[22] Z. Yao, M. Xia, H. Li, T. Chen, Y. Ye, H. Zheng, Bivalve shell: not an abundant useless waste but a functional and versatile biomaterial, Crit. Rev. Environ. Sci. Technol. 44 (22) (2014) 2502–2530, https://doi.org/10.1080/10643389.2013.829763.
[23] H.A. Holland, B.R. Schöne, S. Marali, K.P. Jochum, History of bioavailable lead and iron in the Greater North Sea and Iceland during the last millennium – a bivalve sclerochronological reconstruction, Mar. Pollut. Bull. 87 (1–2) (2014) 104–116, https://doi.org/10.1016/j.marpolbul.2014.08.005.
[24] J. Steinhardt, P.G. Butler, M.L. Carroll, J. Hartley, The application of long-lived bivalve sclerochronology in environmental baseline monitoring, Front. Mar. Sci. 3 (2016) 176, https://doi.org/10.3389/fmars.2016.00176.
[25] E. Cariou, C. Guivel, C. La, L. Lenta, M. Elliot, Lead accumulation in oyster shells, a potential tool for environmental monitoring, Mar. Pollut. Bull. 125 (1–2) (2017) 19–29, https://doi.org/10.1016/j.marpolbul.2017.07.075.
[26] J. Krause-Nehring, T. Brey, S.R. Thorrold, Centennial records of lead contamination in northern Atlantic bivalves (Arctica islandica), Mar. Pollut. Bull. 64 (2) (2012) 233–240, https://doi.org/10.1016/j.marpolbul.2011.11.028.
[27] K.P. Jochum, D. Scholz, B. Stoll, U. Weis, S.A. Wilson, Q. Yang, A. Schwalb, N. Börner, D.E. Jacob, M.O. Andreae, Accurate trace element analysis of speleothems and biogenic calcium carbonates by LA-ICP-MS, Chem. Geol. 318–319 (2012) 31–44, https://doi.org/10.1016/j.chemgeo.2012.05.009.
[28] A. Limbeck, P. Galler, M. Bonta, G. Bauer, W. Nischkauer, F. Vanhaecke, Recent advances in quantitative LA-ICP-MS analysis: challenges and solutions in the life sciences and environmental chemistry ABC Highlights: authored by Rising Stars and Top Experts, Anal. Bioanal. Chem. 407 (22) (2015) 6593–6617, https://doi.org/10.1007/s00216-015-8858-0.

[29] A. Gundlach-Graham, M. Burger, S. Allner, G. Schwarz, H.A.O. Wang, L. Gyr, D. Grolimund, B. Hattendorf, D. Günther, High-speed, high-resolution, multielemental laser ablation-inductively coupled plasma-time-of-flight mass spectrometry imaging: Part I. Instrumentation and two-dimensional imaging of geological samples, Anal. Chem. 87 (16) (2015) 8250–8258, https://doi.org/10.1021/acs.analchem.5b01196.

[30] C. Neff, P. Keresztes Schmidt, P.S. Garofalo, G. Schwarz, D. Günther, Capabilities of automated LA-ICP-TOFMS imaging of geological samples, J. Anal. At. Spectrom. 35 (10) (2020) 2255–2266, https://doi.org/10.1039/d0ja00238k.

[31] D. Günther, B. Hattendorf, Solid sample analysis using laser ablation inductively coupled plasma mass spectrometry, TrAC, Trends Anal. Chem. 24 (3) (2005) 255–265, https://doi.org/10.1016/j.trac.2004.11.017.

[32] E.C. Hathorne, O. Alard, R.H. James, N.W. Rogers, Determination of intratest variability of trace elements in foraminifera by laser ablation inductively coupled plasma-mass spectrometry, G-cubed 4 (12) (2003) 8408, https://doi.org/10.1029/2003GC000539.

[33] M. Elliot, K. Welsh, C. Chilcott, M. McCulloch, J. Chappell, B. Ayling, Profiles of trace elements and stable isotopes derived from giant long-lived Tridacna gigas bivalves: potential applications in paleoclimate studies, Palaeogeogr. Palaeoclimatol. Palaeoecol. 280 (1–2) (2009) 132–142, https://doi.org/10.1016/j.palaeo.2009.06.007.

[34] S. Marali, B.R. Schöne, R. Mertz-Kraus, S.M. Griffin, A.D. Wanamaker, P.G. Butler, H.A. Holland, K.P. Jochum, Reproducibility of trace element time-series (Na/Ca, Mg/Ca, Mn/Ca, Sr/Ca, and Ba/Ca) within and between specimens of the bivalve Arctica islandica – a LA-ICP-MS line scan study, Palaeogeogr. Palaeoclimatol. Palaeoecol. 484 (2017) 109–128, https://doi.org/10.1016/j.palaeo.2016.11.024.

[35] V. Warter, W. Müller, Daily growth and tidal rhythms in Miocene and modern giant clams revealed via ultra-high resolution LA-ICPMS analysis — a novel methodological approach towards improved sclerochemistry, Palaeogeogr. Palaeoclimatol. Palaeoecol. 465 (2017) 362–375, https://doi.org/10.1016/j.palaeo.2016.03.019.

[36] V. Warter, J. Erez, W. Müller, Environmental and physiological controls on daily trace element incorporation in Tridacna crocea from combined laboratory culturing and ultra-high resolution LA-ICP-MS analysis, Palaeogeogr. Palaeoclimatol. Palaeoecol. 496 (2018) 32–47, https://doi.org/10.1016/j.palaeo.2017.12.038.

[37] S. Eggins, P. De Deckker, J. Marshall, Mg/Ca variation in planktonic foraminifera tests: implications for reconstructing -palaeo-seawater temperature and habitat migration, Earth Planet Sci. Lett. 212 (3–4) (2003) 291–306, https://doi.org/10.1016/S0012-821X(03)00283-8.

[38] M. Risk, M. Burchell, K. de Roo, R. Nairn, M. Tubrett, G. Forsterra, Trace elements in bivalve shells from the Río Cruces, Chile, Aquat. Biol. 10 (2010) 85–97, https://doi.org/10.3354/ab00268.

[39] L.D. Pena, E. Calvo, I. Cacho, S. Eggins, C. Pelejero, Identification and removal of Mn-Mg-rich contaminant phases on foraminiferal tests: implications for Mg/Ca past temperature reconstructions, G-cubed 6 (9) (2005) Q09P02, https://doi.org/10.1029/2005GC000930.

[40] Y. Du, F. Lian, L. Zhu, Biosorption of divalent Pb, Cd and Zn on aragonite and calcite mollusk shells, Environ. Pollut. 159 (7) (2011) 1763–1768, https://doi.org/10.1016/j.envpol.2011.04.017.

[41] C. Neff, P. Becker, D. Günther, Parallel flow ablation cell for short signal duration in LA-ICP-TOFMS element imaging, J. Anal. At. Spectrom. 37 (3) (2022) 677–683, https://doi.org/10.1039/d1ja00421b.

[42] Y. Liu, Z. Hu, S. Gao, D. Günther, J. Xu, C. Gao, H. Chen, In situ analysis of major and trace elements of anhydrous minerals by LA-ICP-MS without applying an internal standard, Chem. Geol. 257 (1–2) (2008) 34–43, https://doi.org/10.1016/j.chemgeo.2008.08.004.

[43] L. Hendriks, Microdroplet-Based Calibration for Single-Particle ICP-TOFMS: Fundamentals and Applications, ETH Zurich, 2019. PhD Thesis.

[44] A.C. Larson, R.B. von Dreele, General Structure Analysis System (GSAS), 2000.

[45] B.H. Toby, *EXPGUI*, a graphical user interface for *GSAS*, J. Appl. Crystallogr. 34 (2001) 210–213, https://doi.org/10.1107/S0021889801002242.

[46] ICSD Database , https://icsd.products.fiz-karlsruhe.de/accessed on 16/June/2022.

[47] P.S. Rainbow, D.J.H. Phillips, M.H. Depledge, The significance of trace metal concentrations in marine invertebrates, Mar. Pollut. Bull. 21 (7) (1990) 321–324, https://doi.org/10.1016/0025-326X(90)90791-6.

[48] D.A. Wright, Trace metal and major ion interactions in aquatic animals, Mar. Pollut. Bull. 31 (1–3) (1995) 8–18, https://doi.org/10.1016/0025-326X(95)00036-M.

[49] W.-X. Wang, N.S. Fisher, Modeling metal bioavailability for marine mussels, Rev. Environ. Contam. Toxicol. 151 (1997) 39–95, https://doi.org/10.1007/978-1-4612-1958-3_2.

[50] P.S. Freitas, L.J. Clarke, H. Kennedy, C.A. Richardson, F. Abrantes, Environmental and biological controls on elemental (Mg/Ca, Sr/Ca and Mn/Ca) ratios in shells of the king scallop Pecten maximus, Geochem. Cosmochim. Acta 70 (20) (2006) 5119–5133, https://doi.org/10.1016/j.gca.2006.07.029.

[51] A. Barats, C. Pécheyran, D. Amouroux, S. Dubascoux, L. Chauvaud, O.F.X. Donard, Matrix-matched quantitative analysis of trace-elements in calcium carbonate shells by laser-ablation ICP–MS: application to the determination of daily scale profiles in scallop shell (Pecten maximus), Anal. Bioanal. Chem. 387 (2007) 1131–1140, https://doi.org/10.1007/s00216-006-0954-8.

[52] M. Metian, P. Bustamante, L. Hédouin, M. Warnau, Accumulation of nine metals and one metalloid in the tropical scallop Comptopallium radula from coral reefs in New Caledonia, Environ. Pollut. 152 (3) (2008) 543–552, https://doi.org/10.1016/j.envpol.2007.07.009.

[53] P. Poitevin, L. Chauvaud, C. Pécheyran, P. Lazure, A. Jolivet, J. Thébault, Does trace element composition of bivalve shells record utra-high frequency environmental variations? Mar. Environ. Res. 158 (2020) 104943 https://doi.org/10.1016/j.marenvres.2020.104943.

[54] C. Natali, G. Bianchini, Natural vs anthropogenic components in sediments from the Po River delta coastal lagoons (NE Italy), Environ. Sci. Pollut. Res. 25 (3) (2018) 2981–2991, https://doi.org/10.1007/s11356-017-0986-y.

[55] D. di Giuseppe, L. Vittori Antisari, C. Ferronato, G. Bianchini, New insights on mobility and bioavailability of heavy metals in soils of the Padanian alluvial plain (Ferrara Province, northern Italy), Geochemistry 74 (4) (2014) 615–623, https://doi.org/10.1016/j.chemer.2014.02.004.

[56] K.W. Wong, C.K. Yap, R. Nulit, M.S. Hamzah, S.K. Chen, W.H. Cheng, A. Karami, S.A. Al-Shami, Effects of anthropogenic activities on the heavy metal levels in the clams and sediments in a tropical river, Environ. Sci. Pollut. Res. 24 (2017) 116–134, https://doi.org/10.1007/s11356-016-7951-z.

[57] V. Mouchi, M. de Rafélis, F. Lartaud, M. Fialin, E. Verrecchia, Chemical labelling of oyster shells used for time-calibrated high-resolution Mg/Ca ratios: a tool for estimation of past seasonal temperature variations, Palaeogeogr. Palaeoclimatol. Palaeoecol. 373 (2013) 66–74, https://doi.org/10.1016/j.palaeo.2012.05.023.

[58] M. Lebrato, D. Garbe-Schönberg, M.N. Müller, S. Blanco-Ameijeiras, R.A. Feely, L. Lorenzoni, J.-C. Molinero, K. Bremer, D.O.B. Jones, D. Iglesias-Rodriguez, D. Greeley, M.D. Lamare, A. Paulmier, M. Graco, J. Cartes, J. Barcelos E Ramos, A. de Lara, R. Sanchez-Leal, P. Jimenez, F.E. Paparazzo, S.E. Hartman, U. Westernströer, M. Küter, R. Benavides, A.F. da Silva, S. Bell, C. Payne, S. Olafsdottir, K. Robinson, L.M. Jantunen, A. Korablev, R.J. Webster, E.M. Jones, O. Gilg, P. Bailly du Bois, J. Beldowski, C. Ashjian, N.D. Yahia, B. Twining, X.-G. Chen, L.-C. Tseng, J.-S. Hwang, H.-U. Dahms, A. Oschlies, Global variability in seawater Mg:Ca and Sr:Ca ratios in the modern ocean, Proc. Natl. Acad. Sci. U.S.A. 117 (36) (2020) 22281–22292, https://doi.org/10.1073/pnas.1918943117.

[59] S. Sosdian, D.K. Gentry, C.H. Lear, E.L. Grossman, D. Hicks, Y. Rosenthal, Strontium to calcium ratios in the marine gastropod *Conus ermineus* : growth rate effects and temperature calibration, G-cubed 7 (11) (2006) Q11023, https://doi.org/10.1029/2005GC001233.

[60] C. Jeon, Adsorption behavior of cadmium ions from aqueous solution using pen shells, J. Ind. Eng. Chem. 58 (2018) 57–63, https://doi.org/10.1016/j.jiec.2017.09.007.

[61] A.A. Beni, A. Esmaeili, Biosorption, an efficient method for removing heavy metals from industrial effluents: a Review, Environ. Technol. Innov. 17 (2020) 100503, https://doi.org/10.1016/j.eti.2019.100503.

[62] R.J.R. Monteiro, C.B. Lopes, L.S. Rocha, J.P. Coelho, A.C. Duarte, E. Pereira, Sustainable approach for recycling seafood wastes for the removal of priority hazardous substances (Hg and Cd) from water, J. Environ. Chem. Eng. 4 (1) (2016) 1199–1208, https://doi.org/10.1016/j.jece.2016.01.021.

[63] W. Plazinski, J. Dziuba, W. Rudzinski, Modeling of sorption kinetics: the pseudo-second order equation and the sorbate intraparticle diffusivity, Adsorption 19 (5) (2013) 1055–1064, https://doi.org/10.1007/s10450-013-9529-0.

[64] K.Y. Foo, B.H. Hameed, Insights into the modeling of adsorption isotherm systems, Chem. Eng. J. 156 (1) (2010) 2–10, https://doi.org/10.1016/j.cej.2009.09.013.

[65] M.B. Hay, R.K. Workman, S. Manne, Mechanisms of metal ion sorption on calcite: composition mapping by lateral force microscopy, Langmuir 19 (9) (2003) 3727–3740, https://doi.org/10.1021/la020647s.

[66] R. Allmann, R. Hinek, The introduction of structure types into the inorganic crystal structure database ICSD, Acta Crystallogr. A 63 (5) (2007) 412–417, https://doi.org/10.1107/S0108767307038081.
[67] L. Pan, H. Wang, K. Gu, Nanoliposomes as vehicles for astaxanthin: characterization, in vitro release evaluation and structure, Molecules 23 (11) (2018) 2822, https://doi.org/10.3390/molecules23112822.
[68] L.A. Warren, E.A. Haack, Biogeochemical controls on metal behaviour in freshwater environments, Earth Sci. Rev. 54 (4) (2001) 261–320, https://doi.org/10.1016/S0012-8252(01)00032-0.
[69] A. García-Sánchez, E. Âlvarez-Ayuso, Sorption of Zn, Cd and Cr on calcite. Application to purification of industrial wastewaters, Miner. Eng. 15 (7) (2002) 539–547, https://doi.org/10.1016/S0892-6875(02)00072-9.
[70] D.L. Bish, J.E. Post, Modern Powder Diffraction, vol. 20, Walter de Gruyter GmbH & Co KG, 2018.
[71] A.F. Gualtieri, A guided training exercise of quantitative phase analysis using EXPGUI. GSAS Tutorials and Examples, 2003.
[72] R.D. Shannon, C.T. Prewitt, Revised values of effective ionic radii, Acta Crystallogr. B 26 (1970) 1046, https://doi.org/10.1107/S0567740870003576.
[73] A. Janeković, E. Matijević, Preparation of monodispersed colloidal cadmium compounds, J. Colloid Interface Sci. 103 (2) (1985) 436–447, https://doi.org/10.1016/0021-9797(85)90120-1.
[74] G. Bultosa, A.M. Mulokozi, Kinetics of the thermal decomposition of cadmium carbonate (CdCO3), J. Therm. Anal. 45 (1995) 1339–1348, https://doi.org/10.1007/BF02547428.
[75] C. Yuan, Z. Jin, X. Xu, H. Zhuang, W. Shen, Preparation and stability of the inclusion complex of astaxanthin with hydroxypropyl-β-cyclodextrin, Food Chem. 109 (2) (2008) 264–268, https://doi.org/10.1016/j.foodchem.2007.07.051.
[76] S.T. Williams, Molluscan shell colour, Biol. Rev. 92 (2) (2017) 1039–1058, https://doi.org/10.1111/brv.12268.
[77] W. Barnard, D. de Waal, Raman investigation of pigmentary molecules in the molluscan biogenic matrix, J. Raman Spectrosc. 37 (1–3) (2006) 342–352, https://doi.org/10.1002/jrs.1461.
[78] G.D. Rosenberg, Calcium concentration in the shell of the bivalve Chione undatella sowerby, Nature 244 (1973) 155–156, https://doi.org/10.1038/244155a0.
[79] A.L. Soldati, D.E. Jacob, U. Wehrmeister, T. Häger, W. Hofmeister, Micro-Raman spectroscopy of pigments contained in different calcium carbonate polymorphs from freshwater cultured pearls, J. Raman Spectrosc. 39 (4) (2008) 525–536, https://doi.org/10.1002/jrs.1873.
[80] C.M. Thompson, E.W. North, S.N. White, S.M. Gallager, An analysis of bivalve larval shell pigments using micro-Raman spectroscopy, J. Raman Spectrosc. 45 (5) (2014) 349–358, https://doi.org/10.1002/jrs.4470.
[81] D. Gaspard, C. Paris, P. Loubry, G. Luquet, Raman investigation of the pigment families in recent and fossil brachiopod shells, Spectrochim. Acta Mol. Biomol. Spectrosc. 208 (2019) 73–84, https://doi.org/10.1016/j.saa.2018.09.050.
[82] C. Hedegaard, J.-F. Bardeau, D. Chateigner, Molluscan shell pigments: an in situ resonance Raman study, J. Molluscan Stud. 72 (2006) 157–162, https://doi.org/10.1093/mollus/eyi062.
[83] N.E. Polyakov, A.L. Focsan, M.K. Bowman, L.D. Kispert, Free radical formation in novel carotenoid metal ion complexes of astaxanthin, J. Phys. Chem. B 114 (50) (2010) 16968–16977, https://doi.org/10.1021/jp109039v.
[84] E. Hernández-Marin, A. Barbosa, A. Martínez, The metal cation chelating capacity of astaxanthin. Does this have any influence on antiradical activity? Molecules 17 (1) (2012) 1039–1054, https://doi.org/10.3390/molecules17011039.